Biostratigraphic evidence for dramatic Holocene uplift of Robinson Crusoe Island, Juan Fernández Ridge, SE Pacific Ocean

P. Sepúlveda[1], J. P. Le Roux[1,2], L.E. Lara[3 *], G. Orozco[3,2,1], V. Astudillo[1]

[1]{Departamento de Geología, FCFM, Universidad de Chile}

[2]{Centro de Excelencia en Geotermia de los Andes, Santiago, Chile}

[3]{Volcano Hazards Program, Servicio Nacional de Geología y Minería, Santiago, Chile}

Correspondance to: Luis E. Lara (luis.lara@sernageomin.cl)

Abstract

Hotspot oceanic islands typically experience subsidence due to several processes related to migration of the oceanic plate away from the mantle plume and surface flexural loading. However, many other processes can interrupt subsidence, some of which may be associated with catastrophic events. A study of the biostratigraphy and sedimentology of Holocene deposits on Robinson Crusoe Island (RCI) on the Juan Fernández Ridge indicated that dramatic uplift occurred since 8,000 years BP, at a rate of about 8.5 mm yr^{-1}. This is evidenced by supratidal flats with tepee structures and sand layers containing marine gastropods (mostly *Nerita* sp.) that are now exposed ca. 70 m a.s.l. The active hotspot is located 280 km further west and the last volcanic activity on RCI occurred at ca. 800,000 years BP. Long-term subsidence is evidenced by deep submerged marine abrasion terraces at RCI. As no direct evidence was found for the existence of a compensating bulge generated by the present hotspot upon which RCI would be situated, it must be concluded that subsidence in the wake of the migrating mantle plume was interrupted by very rapid uplift, but on a scale that did not fully compensate for the previous subsidence. This can be attributed to large-scale landslides followed by isostatic rebound, although this is only vaguely reflected in the low-resolution bathymetry of the area. To determine if this

mechanism produced the uplift, a detailed bathymetric survey of the area will be required. If such a survey confirms this hypothesis, it may have implications for the short-term dynamics of vertical variations of oceanic edifices and their related effects on ecosystems and human population.

1 Introduction

Oceanic hotspots are relatively mantle-fixed and localized volcanic sources, which transport rising magmas through oceanic lithosphere. As the plates move away due to sea-floor spreading, oceanic volcanoes are extinguished and new volcanic edifices arise over the active hotspot, forming age-progressive island chains such as the Hawaiian-Emperor seamount chain.

A conspicuous feature of hotspot oceanic islands is their complex history of vertical displacement (e.g., Ramalho et al., 2013). As earlier noted by Charles Darwin in the 19th century, these vertical movements respond to a number of large-scale processes known at present to be related to the growth and decay of the underlying swell (Ramalho et al., 2010a), flexural loading (Watts and ten Brink, 1989), isostatic rebound (Smith and Wessel, 2000), bulging effects resulting from loading of nearby islands and seamounts (e.g., Bianco et al., 2005), density changes in the mantle, intrusions at the base of the edifice (e.g., Klügel et al., 2005) and gradual cooling of the lithosphere (Stein and Stein, 1992).

Although most of the present oceanic islands are subsiding (such as Surtsey Island over the last decades; e.g., Moore et al., 1992), other processes such as those mentioned above and especially catastrophic events like giant landslides can also trigger sudden uplift, as inferred for archetypical hotspot volcanoes such as Hawaii (e.g., Smith and Wessel, 2000). It is therefore important to identify such mechanisms and their possible short- or long-term effects, especially for those few cases where they occur at very high rates.

Vertical movements at Juan Fernández Ridge, located on the relatively fast-moving Nazca Plate (Gripp and Gordon, 2002) are still poorly known due to the general absence of detailed bathymetry and other known subsidence or uplift tracers. In this context, the record of local sea-level changes is a tool to better understand the uplift/subsidence history in different geological settings (e.g., Toomey et al., 2013; Jara and Melnick, 2015). Here we present biostratigraphic and sedimentological evidence for a very high Holocene uplift rate of RCI and discuss possible mechanisms with implications for the future evolution of this oceanic island.

2 Material and Methods

2.1 Geological and geomorphological background

The Juan Fernández Ridge (JFR), located on the Nazca Plate in the Pacific Ocean off central Chile (Fig. 1), is an 800 km long seamounts and volcanic islands chain extending E-W at latitude 33°S. It has been interpreted as the expression of a fixed hotspot (Von Heune et al., 1997; Montelli et al., 2006) related to a primary mantle plume in the sense of Courtillot et al. (2003) or as part of a 'hot line' (Bonatti et al., 1977).

JFR is largely formed by the Miocene (ca. 9 million years BP) O´Higgins guyot and seamount (Von Heune et al., 1997), with lavas dating back to ca. 4 million years BP on RCI and nearby Santa Clara Island (Fig. 1), and ca. 1 million years BP on Alejandro Selkirk Island about 120 km away (Farley et al., 1993). The relief on the western, arid part of RCI is characterized by coastal cliffs bordering a terrace at about 70 m a.s.l., which is especially well developed in the southwestern panhandle (Fig. 1). This terrace is formed on top of a middle Pleistocene age (ca. 800,000 years BP), post-shield volcanic platform from which pyroclastic cones emerge reaching a maximum elevation of 915 m (Lara et al., 2013). Holocene sedimentary deposits are restricted to the terrace in the vicinity of Bahía Tierra Blanca (Spanish for "White Land Bay"). The latter name is applied to a succession described by Morales (1987) as poorly consolidated, calcareous sandstones at the base grading upward into tuffaceous sandstones with numerous fossils. In the transition zone are *Acanthina* and *Lima* fossils with bryozoa fragments, whereas the tuffaceous sandstones host *Luccinea*, *Distoechia*, *Bythinia*, *Orcula*, *Tropicorbis*, *Ena*, and *Cyrena* spp. indicating a Pleistocene-Holocene age, based on a similar fossil assemblage on the continent at this latitude (Covacevich, 1971; Valenzuela, 1978). The Bahía Tierra Blanca succession has its base at a variable elevation but generally at ca. 70 m above the present mean sea level, where active, incipient barchan dunes (Morales, 1987), partially rework the succession described above.

Robinson Crusoe Island (RCI) has at least two submerged marine abrasion terraces, with edges at ca. 200 m and ca. 500 m b.s.l. (Astudillo, 2014). The present depth of these originally shallow features suggests long-term subsidence of this volcanic edifice.

2.2 Methods

Field campaigns were carried out on RCI in 2011-2013, during which geological mapping was undertaken, stratigraphic sections were measured, and samples were collected for further analysis. Laboratory work consisted of fossil identification, petrographic microscopy, sieve and Mastersizer 2000 (Malvern Instruments, Malvern, United Kingdom) analysis of the sediment grain-size distribution, and radiocarbon dating (Beta Analytic Inc., Miami, Accelerator Mass Spectrometer) of gastropods. The latter were collected mostly from sites 1 and 5 (Fig.1). Several specimens were hand-picked from bulk samples and three were selected for dating based on their stratigraphic position and systematics. AMS radiocarbon dates were first corrected for the global marine reservoir effect (e.g., Ulm, 2006) with the Marine IntCal09 calibration program (Reimer et al., 2009). For the localized reservoir correction a Delta-R value of 373±76 from a nearby site was used (Marine Reservoir Correction, 2012). Elevations were measured with a dGPS Trimble®NetRS® and barometric altimeters with respect to the current sea-level and corrected for the regional sea level and daily variation (Tabla de Marea, 2012) with a nominal uncertainty of 5 m. In order to determine thresholds for the wind velocity capable of moving collected fossils we used the formula in Appendix A, mostly based on Le Roux (2005).

3 Results

3.1 Depositional environments

Four lithostratigraphic units and three lithofacies were identified in the Bahía Tierra Blanca succession, which reaches a total thickness between 2 and 4 m at any specific locality (Fig. 2).

Unit 1 is largely composed of facies 1, which discordantly overlies weathered, basaltic lavas. It consists of very poorly consolidated, slightly calcareous, reddish brown to reddish purple deposits ranging in size from very fine sandstone to claystone. Their composition is made up of volcanic ash mixed with the underlying, weathered lava material. These deposits contain up to 2% bioclasts (mostly marine bivalves) together with pellets. The most striking feature of this facies is ubiquitous teepee structures up to 1 m in diameter, which display prominent edges elevated 3-5 cm above the central parts (Fig. 2). The cracks have been filled in by sands from the overlying unit. Locally, shallow channels and rill marks are present.

While the reddish to purplish brown color suggests a mainly subaerial environment, the presence of teepee structures with elevated rims indicate frequent flooding and drying cycles. These, as well as the occurrence of pellets, are typical of supratidal flats (e.g., Assereto and Kendall, 1977), which concurs with the presence of shallow channels probably reflecting tidal creeks. The general scarcity of hard-shell fossils in this facies can be interpreted as representing a generally hostile environment subjected to frequent dry periods between spring high tides, followed by seawater flooding that would kill land-dwelling snails and other organisms. Marine shells washed in during spring high tides would probably accumulate along the shoreline. Soft-bodied forms more tolerant to such conditions, on the other hand, would not be preserved in such an oxidizing environment.

Facies 2 is present in units 2 and 3, which differ mainly in the darker brown color of the latter due to a thin brownish film coating the grains. Both units 2 and 3 show large-scale, low angle planar cross-bedding and horizontal lamination, but in unit 3, high-angle planar and trough cross-bedding are locally present. The 1-2 cm thick cross-beds are formed by alternating light and darker-colored grains without any evident gradation. Rhizocretions are present in the uppermost parts of both units, where individual forms may reach 1.5 m in length (Fig. 2). Although rhizocretions and vertebrate burrows are generally rare, some parts have a fairly high density of the former. Unit 2 is capped locally by whitish calcrete indicating incipient pedogenesis. Gastropods such as *Succinea*, *Fernandezia*, and *Nerita* occur in the middle to upper part of unit 2. Petrographically, the sandstone is well sorted with subrounded grains, lacking a matrix, and cement being only locally present. Bioclasts compose around 55% of the rock, including brachiopod and pelecypod fragments, echinoderm spines, bryozoa, red algae, foraminifers, and sub-rounded pellets. The rest of the composition is made up of volcanic fragments and minerals such as K-feldspar, plagioclase, clinopyroxene, and olivine, with rare quartz. Grain-size analysis of several samples from this facies shows a small traction load, a prominent and very well-sorted saltation load, and a medium- to well-sorted suspension load. This facies was interpreted as reflecting coastal eolian deposits perhaps locally affected by weak wave action. This is supported by the reddish brown color of the sandstones, their predominantly fine grain-size with cumulative curves typical of wind-blown deposits, and the presence of the land-dwelling snails *Succinea* and *Fernandezia*, as well as root and burrow systems. The horizontally laminated strata probably formed in sand sheets between low dunes, which might have been parabolic in shape as suggested by the dominance of low-angle planar cross-bedding. Some were subsequently converted into dikaka dunes (Glennie and Evamy, 1968) by vegetation. Some low-angle cross-bedding might represent reworking by dissipated wave action during storms and spring high tides along the landward edges of wide supratidal flats. This could also explain the presence of thick-shelled *Nerita* (a marine species) in Unit 2. The presence of fragmented marine invertebrates indicates a marine source for most of these sands, which suggests that they formed at a low elevation above sea level.

Facies 3 is composed of greyish white, medium sorted sandstones interbedded with gravel. The sandstones consist of bioclasts (45-57%) mostly represented by marine shell fragments including bivalves, gastropods such as *Succinea*, bryozoa, algae, and foraminifers, together with lithic volcanic fragments (27-45%) and volcanic minerals such as pyroxene, olivine, and felsic minerals (10-17%). The gravels are greyish brown and matrix- to clast-supported, with the clasts reaching up to 5 cm in diameter. They are mainly volcanic and angular. Locally, calcretes are present at the top of this facies. This facies clearly represents fluvial deposits, probably consisting of shallow, quick-flowing ephemeral streams with gravelly channels and sandy bars. These most likely drained exposed basalts on the fringes of the eolian sand sheets, but also reworked the latter to incorporate the marine bioclasts.

3.2 Radiocarbon dating

Specimens of *Nerita* (Fig. 3) from the eolian sandstones of unit 2 yielded calibrated radiocarbon ages between 8,320 and 8,030 BP (conventional radiometric age of 7,860±40 years BP). Values corrected for the global marine reservoir effect (with a local Delta-R of 373±76 as obtained for the similar entry at http://radiocarbon.pa.qub.ac.uk/marine/ correspond to 7,550±90 years BP (see Table 1). These marine species were probably reworked from the supratidal flats of unit 1 and would thus represent the age of the latter. On the other hand, land-dwelling species as *Succinea* and *Fernandezia* (e.g., Odhner, 1922) from units 3 and 4 gave calibrated radiocarbon ages between 5,440 and 5,090 years BP (4,580±30 conventional years BP) and 7,680 and 7,580 years BP (6,790±40 conventional years BP), respectively.

4 Discussion

The stratigraphic succession of the Bahía Tierra Blanca deposits suggests that supratidal conditions existed in the southwestern panhandle of RCI between 8,320 and 8,030 years BP (horizons with *Nerita*). It is unlikely that the tides reached more than 1-2 m above the mean sea level, because topographic tide-enhancing conditions such as funnel-shaped estuaries could not have existed due to the absence of large rivers on this part of the island. These supratidal flats were encroached upon by eolian coastal plain deposits at around 5,430 years BP (horizons with *Succinea* and *Fernandezia*) and finally fluvial sedimentation as the sea-level receded further during the late Holocene Climatic Optimum (Davis et al., 2003; Koshkarova and Koshkarov, 2004), when the southwestern panhandle would have received more rain. The present elevation of the supratidal deposits on a marine terrace at 70 m a.s.l. indicates a very rapid relative sea-level fall since that time. Furthermore, it can be assumed that the eolian deposits of units 2 and 3 were also not more than a few meters above the tidal flats, as they had apparently been reworked locally by waves. This is supported by the low-angle cross-bedding typical of beaches and the presence of reworked *Nerita*. The latter could not have been blown uphill by wind, considering that they reach up to 1 cm in diameter (Appendix A). Assuming that they were not more than 2 m above the tidal flats or beaches, a relative sea-level fall of at least 8.5 mm yr^{-1} is implied.

Eustatic sea-levels have been well below the present-day level over the last 20,000 years (Bindoff et al., 2007; Fleming et al., 1998). In Tahiti and almost all other regions of the world where detailed records exist (e.g., Lambeck et al., 2002), there are indications that the sea-level at 8,000 years BP was about 15 m below that of the present (Fleming et al., 1998; Milne et al., 2005). This rules out an eustatic highstand at the time. A mean uplift rate of around 8.5 mm yr^{-1} is extremely high, considering that the average rate of uplift of the Andes has been only about 0.2-0.3 mm yr^{-1} since the Late Miocene (Gregory-Wodzicki, 2000) and uplift rates of other oceanic islands were < 0.33 mm yr^{-1} (e.g., in the oldest Hawaiian islands as reported by McMurtry et al., 2004 and references therein). Oceanic islands with evidence of significant freeboard (e.g. Cape Verde) show uplift rates <0.4 mm yr^{-1} (Ramalho et al., 2010a; 2010b). This high vertical displacement rate is only comparable with the subsidence rate of the active Hawaii Island, which sinks at ca. 2.6 mm yr^{-1} (McMurtry et al., 2004).

The dramatic Holocene uplift of RCI cannot be explained as a flexural response to the loading exerted by the edifices created by the active hotspot. Isobaths (after Becker et al., 2009; see also Rodrigo and Lara, 2014) show that the sea floor north of the JFR descends from 3,800 m b.s.l. northwest of Alejandro Selkirk to about 4,000 m b.s.l. north of the latter, from where it declines further to reach 4,200 m b.s.l. north of RCI and 4,300 m b.s.l. northeast thereof. There is thus no direct evidence for the existence of a bulge upon which RCI would be situated. The bathymetry in fact shows a negative anomaly for this part of the oceanic crust, which suggests that subsidence did take place, but was partially reversed by a subsequent process commencing at about 8,000 BP. General subsidence normally occurs in the wake of a mantle plume migrating away from a particular area, as this part of the lithosphere would no longer be sustained by it, combined with the load exerted by the shield volcano. The generation of new islands and seamounts above a fixed mantle plume could also cause loading and subsidence of the crust accompanied by the formation of an adjacent, compensating bulge, and hence local uplift. However, a theoretical bulge caused by the youngest volcanism at the Friday/Domingo seamounts (250 km further west of RCI) is not enough to explain uplift at RCI if realistic values for elastic parameters are considered (e.g., Manríquez et al., 2013). Watts and ten Brink (1989), e.g., proposed the existence of such a bulge 300 km from the present hotspot on Hawaii Island, which formed in response to subsidence of 1,300 m at the latter locality over the last 500,000 years (McMurtry et al., 2010). Evidence of >20 m uplift is found at Oahu in the now emerged coral reefs (McMurtry et al., 2010). Nevertheless, there is no evidence of recent Holocene volcanism further west at a distance short enough to promote uplift at RCI. In addition, 3D modeling of the lithospheric flexure seaward of the trench (Manríquez et al., 2013) shows that even more complex loads (seamount loading, bending of the lithosphere near the trench and sedimentary fill inside the trench south of 34°S) do not generate a flexural response beyond 350 km from the outer rise.

Intrusion at the base of the edifice, as proposed for the Canary Islands (Klügel et al., 2005) and Cape Verde (Madeira et al., 2010; Ramalho et al., 2010b) cannot be ruled out. However, because of the absence of volcanism younger than ca. 1 million years BP and the rapid displacement of the Nazca Plate, we have a reasonable doubt about the occurrence of this process in the Holocene.

Another possibility could be the development of large-scale landslides. The southwestern part of the island is characterized by steep coastal cliffs, and the area lies opposite Santa Clara Island that is thought to have originally formed part of a larger island incorporating RCI (Danton, 2004). The region between the two islands might have experienced a large-scale landslide event (or events), which in turn may have caused isostatic rebound. The latter is thought to be larger on oceanic plates than on continental plates because of their more limited thickness. In hotspot environments and other high heat-flow areas such as spreading boundaries the asthenosphere should be less viscous, so that rebound rates may increase. Similar events have been reported in Hawaii during the last 2 m.y. (McMurtry et al., 2004). Smith and Wessel (2000) calculated that the removal of 800 km^3 of material during the Alika landslide elevated the adjacent terrain by about 17 m, whereas McMurtry et al. (2004) calculated uplift of 109 m for a volume of 5,000 km^3 removed during the Nuuanu landslide. Taking into account an elastic thickness of ca. 10 km (Manríquez et al., 2013), about 1,000 km^3 of material (ca. 15% of the initial volume) would thus have had to be removed to account for ca. 70 m of uplift at RCI. Such a large mass wasting deposit is not evident in the low resolution bathymetry around the RCI, but the caldera-like structure open to the south and some rough relief on the distal flanks suggest that a landslide is a plausible hypothesis.

5 Conclusions

Biostratigraphic evidence for the exposure of former supratidal flats 70 m above the present sea level on RCI could be related to a large Holocene landslide not previously detected. Large-scale landslides around oceanic islands can probably be attributed to an increase in local slopes generated by the construction of volcanic edifices and the development of rifting. At RCI there has been no major surface volcanic activity since about 3 Ma, with only minor post-shield activity at 800,000 years BP (Lara et al., 2013). Nevertheless, the topography of RCI is even steeper than that of Hawaii, which could have allowed large-scale sliding to take place. As modeled by Smith and Wessel (2000), directed giant landslides generate isostatic rebound which is larger over the failed flank and spatially asymmetric. Catastrophic landslides can generate tsunamis in addition to directly affecting large parts of the island itself. The steep slopes on and around the island, its volcanic composition (notorious for rapid weathering and soil production), and the frequency of large earthquakes along the East Pacific rim, are factors that make such landslides more likely. It is therefore important that a detailed bathymetric survey of the area around RCI be carried out to detect possible Holocene landslide scars and deposits. If such a survey confirms this hypothesis, it may have implications for the short-term dynamics affecting vertical variations of oceanic edifices. These findings highlight the importance of biological markers as tools to better understand sea-level changes and the complex evolution of oceanic islands.

Acknowledgements

This research was initially supported by Fondecyt 1110966 project granted to L.E. Lara and is also part of a collaborative effort to better understand fundamental processes in the oceanic islands of the Nazca Plate, now with funding from Fondecyt 1141303 project. J.P. Le Roux and G. Orozco worked under the auspices of Project CONICYT/FONDAP/15090013. J.C. Baez kindly provided dGPS equipment and data reduction. S.N. Nielsen and S. Letelier advised on the fossil record. CONAF authorized scientific research in this protected area and DIFROL provided logistical support during the last 2013 field campaign. Comments by R. Ramalho, an anonymous referee and associate editor B.J. Sigurdsson are greatly appreciated.

References

Assereto, R. L. A. M., and Kendall, C. G. St C.: Nature, origin and classification of peritidal tepee structures and related breccias, Sedimentology, 24, l53-2l0, doi:10.1111/j.1365-3091.1977.tb00254.x, 1977.

Astudillo, V.: Geomorfología y evolución geológica de la isla Robinson Crusoe, Archipiélago Juan Fernández: Memoria de Título (unpublished thesis), Universidad de Chile, Santiago, 2014.

Audley-Charles, M. G.: Rates of Neogene and Quaternary tectonic movements in the Southern Banda Arc based on micropalaeontology. J. Geo. Soc. London 143,161-175, doi:10.1144/gsjgs.143.1.0161, 1986.

Becker, J. J., Sandwell, D. T., Smith, W. H. F., Braud, J., Binder, B., Depner, J., and Weatherall, P.: Global bathymetry and elevation data at 30 arc seconds resolution: SRTM30_PLUS, Mar. Geod,, 32, 355-371, doi: 10.1080/01490410903297766, 2009.

Bianco, T. A., Ito, G., Becker, J. M., and García, M. O.: Secondary Hawaiian volcanism formed by flexural arch decompression, Geochem. Geophys. Geosyst., 6, Q08009, doi:10.1029/2005GC000945, 2005.

Bindoff, N. L., Willebrand, J., Artale, V., Cazenave, A., Gregory, J., Gulev, S., Hanawa, K., Le Quéré, C., Levitus, S., Nojiri, Y., Shum, C. K., Talley, L. D., and Unnikrishnan, A.: Observations: Oceanic Climate Change and Sea Level, in: Climate Change 2007: The Physical Science Basis, Contribution of Working Group I to the Fourth Assessment

Report of the Intergovernmental Panel on Climate Change [Solomon, S., Qin, D., Manning, M., Chen, Z., Marquis, M., Averyt, K. B., Tignor, M., and Miller, H. L. (eds.)], Cambridge University Press, Cambridge, United Kingdom and New York, NY, USA, 2007.

Bonatti, E., Harrison, C. G. A., Fisher, D. E., Honnorez, J., Schilling, J. -G., Stipp, J. J., and Zentilli, M.: Easter volcanic chain (southeast Pacific): A mantle hot line. J. Geophys. Res., 82, 2457-2478, doi: 10.1029/JB082i017p02457, 1977.

Courtillot, V., Davaille, A., Besse, J., and Stock, J.: Three distinct types of hotspots in the Earth´s mantle, Earth Planet. Sci. Lett., 205, 295-308, doi:10.1016/S0012-821X(02)01048-8, 2003.

Covacevich, V.: Los moluscos pleistocénicos y holocénicos de San Vicente de Tagua Tagua: Memoria de Título (unpublished thesis), Universidad de Chile, Santiago, 1971.

Danton, P. H.: Plantas silvestres de la isla Robinson Crusoe: Guía de Reconocimiento, Corporación Nacional Forestal, Región de Valparaíso, Viña del Mar, 2004.

Davis, B. A. S., Brewer, S., Stevenson, A. C., and Guiot, J.: The temperature of Europe during the Holocene reconstructed from pollen data, Quaternary Sci. Rev., 22, 1701-1716, doi:10.1016/S0277-3791(03)00173-2, 2003.

Farley, K. A., Basu, A. R., and Craig, H.: He, Sr and Nd isotopic variations in lavas from the Juan Fernandez Archipelago, SE Pacific, Contrib. Mineral Petr., 115, 75-87, doi:10.1007/BF00712980, 1993.

Fleming, K., Johnston, P., Zwartz, D., Yokoyama, Y., Lambeck, K., and Chappell, J.: Refining the eustatic sea-level curve since the Last Glacial Maximum using far- and intermediate-field sites, Earth Planet. Sci. Lett., 163, 327-342, doi:10.1016/S0012-821X(98)00198-8, 1998.

Foulger, G. R.: Plates vs. Plumes: A Geological Controversy, Wiley-Blackwell, New York, 364 pp., 2010.

Glennie, K.W., and Evamy, B.D.: Dikaka: Plants and plant-rot structures associated with Aeolian sand, Palaeogeogr. Palaeocl, 4.2, doi:10.1016/0031-0182(68)90088-6, 77-87, 1968.

Gregory-Wodzicki, K. M.: Uplift history of the Central and Northern Andes: A review, Geol. Soc. Am. Bull., 112, 1091-1105, doi:10.1130/0016-7606(2000)1122.3.CO;2, 2000.

Gripp, A. E., and Gordon R. G.: Young tracks of hotspots and current plate velocities, Geophys. J. Int., 150, 321-361, doi:10.1046/j.1365-246X.2002.01627.x, 2002.

Jara, J. and Melnick, D.: Unraveling sea-level variations and tectonic uplift in wave-built marine terraces, Santa María Island, Chile, Quaternary Res., 83, 216-228, doi:10.1016/j.yqres.2014.10.002, 2015.

Klügel, A., Hansteen, T. H., and Galipp, K.: Magma storage and underplating beneath Cumbre Vieja volcano, La Palma (Canary Islands). Earth Planet. Sci. Lett., 236,211–226, doi:10.1016/j.epsl.2005.04.006, 2005.

Koshkarova, V. L., and Koshkarov, A. D.: Regional signatures of changing landscape and climate of northern central Siberia in the Holocene, Russ. Geol. Geophys., 45, 672-685, 2004.

Lambeck, K., Yokoyama, Y., and Purcell, T.: Into and out of the Last Glacial Maximum: sea-level change during Oxygen Isotope Stages 3 and 2, Quaternary Sci. Rev., 21, 343-360, doi:10.1016/S0277-3791(01)00071-3, 2002.

Lara, L. E., Reyes, J., Piña-Gauthier, M., and Orozco, G.: Geological evidence of a post shield stage at the Juan Fernandez Ridge, Nazca Plate, IAVCEI Scientific Assembly Kagoshima, Abstracts, 2013.

Le Roux, J. P.: Grains in motion: A review, Sediment. Geol., 178, 285-313, doi:10.1016/j.sedgeo.2005.05.009, 2005.

Le Roux, J. P., Gutiérrez, N. M., Hinojosa, L. F., Pedroza, V., Becerra, J.: Reply to Comment of Encinas et al. (2014) on: ‘Evidence for an Early-Middle Miocene age of the Navidad Formation (central Chile): Paleontological, climatic and tectonic implications’ of Gutiérrez et al. (2013, Andean Geol. 40 (1), 66-78). Andean Geol., 41, 657-669, doi:10.5027/andgeoV41n3-a08, 2014.

Madeira, J., Mata, J., Mourão, C., Brum da Silveira, A., Martins, S., Ramalho, R. S., and Hoffmann, D. L.: Volcano-stratigraphic and structural evolution of Brava Island (Cape Verde) from ^{40}Ar/^{39}Ar, U-Th and field constraints. J. Volcanol. Geoth. Res., 196, 219–235, doi:10.1016/j.jvolgeores.2010.07.010, 2010.

Manríquez, P., Contreras-Reyes, E., and Osses, A.: Lithospheric 3-D flexure modelling of the oceanic plate seaward of the trench using variable elastic thickness, Geophys. J. Int., 196, 681-693, doi: 10.1093/gji/ggt464, 2014.

Marine Reservoir Correction: http://radiocarbon.pa.qub.ac.uk/marine/, last access: 2012.

McMurtry, G. M., Watts, P., Fryer, G. J., Smith, J. R., and Imamura, F.: Giant landslides, mega-tsunamis, and paleo-sea level in the Hawaiian Islands, Mar. Geol., 203, 219-233, doi:10.1016/S0025-3227(03)00306-2, 2004.

McMurtry, G. M., Campbell, J. F., Fryer, G. J., and Fietzke, J.: Uplift of Oahu, Hawaii, during the past 500 k.y. as recorded by elevated reef deposits, Geology, 38, 27-30, doi:10.1130/G30378.1, 2010.

Milne, G. A., Long, A. J., and Bassett, S. E.: Modelling Holocene relative sea-level observations from the Caribbean and South America, Quaternary Sci. Rev., 24, 1183-1202, doi:10.1016/j.quascirev.2004.10.005, 2005.

Montelli, R., Nolet, G., Dahlen, F. A., and Masters, G.: A catalogue of deep mantle plumes: New results from finite-frequency tomography, Geochem. Geophy. Geosyst., 7, Q11007, doi:10.1029/2006GC001248, 2006.

Moore, J. G., Jakobsson, S., and Holmjarn, J.: Subsidence of Surtsey Volcano, 1967-1991, B.Volcanol., 55, doi:10.1007/BF00301116, 1992.

Morales, A.: Geología de las islas Robinson Crusoe y Santa Clara, Archipiélago de Juan Fernández, V. Región, Chile: Memoria de Título (unpublished thesis), Universidad Católica del Norte, Antofagasta, 1987.

Odhner, N.: Mollusca from Juan Fernández and Easter Island, Addenda, in: The Natural History of Juan Fernández and Easter Island, Skottsberg, C. (ed.), Almqvist and Wiksells Boktryckeri, Uppsala1922.

Price, N. J., Audley-Charles, M. G.: Tectonic collision processes after plate rupture, Tectonophysics, 140, 121-129, doi:10.1016/0040-1951(87)90224-1, 1987.

Ramalho, R. S., Helffrich, G., Cosca, M., Vance, D., Hoffmann, D. and Schmidt, D. N.: Episodic swell growth inferred from variable uplift of the Cape Verde hotspot islands, Nat. Geosci., 3,774–777, doi:10.1038/ngeo982, 2010a.

Ramalho, R. S., Helffrich, G. R., Schmidt, D. N., and Vance, D.: Tracers of uplift and subsidence in the Cape Verde Archipelago. J.Geol. Soc. London, 167, 519–538, doi:10.1144/0016-76492009-056, 2010b.

Ramalho, R. S., Quartau, R., Trenhaile, A. S., Mitchell, N. C., Woodroffe, C. D., and Ávila, S. P.: Coastal evolution on volcanic oceanic islands: A complex interplay between volcanism, erosion, sedimentation, sea-level change and biogenic production, Earth- Sci. Rev., 127, 140-170, doi:10.1016/j.earscirev.2013.10.007, 2013.

Reimer, P. J., Baillie, M. G. L., Bard, E., Bayliss, A., Beck, J. W., Blackwell, P. G., Bronk Ramsey, C., Buck, C. E., Burr, G. S., Edwards, R. L., Friedrich, M., Grootes, P. M., Guilderson, T. P., Hajdas, I., Heaton, T. J., Hogg, A. G., Hughen, K. A., Kaiser, K. F., Kromer, B., McCormac, F. G., Manning, S. W., Reimer, R. W., Richards, D. A., Southon, J. R., Talamo, S., Turney, C. S. M., van der Plicht, J., and Weyhenmeyer, C. E.: IntCal09 and Marine09 radiocarbon age calibration curves, 0-50,000 years cal BP, Radiocarbon, 51, 1111-1150, 2009.

Rodrigo, C. and Lara, L. E.: Plate tectonics and the origin of the Juan Fernández Ridge: analysis of bathymetry and magnetic patterns, Lat. Am. J. Aquat. Res., 42, 907-917, doi:10.3856/vol42-issue4-fulltext-15, 2014.

Smith, J. R., and Wessel, P.: Isostatic consequences of giant landslides on the Hawaiian Ridge, Pure Appl. Geophys., 157, 1097-1114, doi: 10.1007/s000240050019, 2000.

Stein, C. and Stein, S.: A model for the global variation in oceanic depth and heat flow with lithospheric age, Nature, 359, 123-129, doi:10.1038/359123a0, 1992.

Tabla de Marea, SHOA: http://www.shoa.cl/mareas/tablademarea.html, last access: 2012.

Toomey, M., Ashton, A.D., and Perron, J.T.: Profiles of ocean island coral reefs controlled by sea-level history and carbonate accumulation rates, Geology, 41, 731-734, doi:10.1130/G34109.1, 2013.

Ulm, S.: Australian marine reservoir effects: A guide to ΔR values, Aust. Archaeol., 63, 57-60, 2006.

Valenzuela, E.: Pleistoceno marino en la isla Robinson Crusoe, Comunicaciones, 22, 32-35, 1978.

Von Heune, R., Corvalán, J., Flueh, E. R., Hinz, K., Korstgard, J., Ranero, C. R., and Weinrebe, W.: Tectonic control of the subducting Juan Fernández Ridge on the Andean margin near Valparaíso, Chile, Tectonics, 16, 474-488, doi:10.1029/96TC03703, 1997.

Watts, A. B. and ten Brink, S.: Crustal structure, flexure, and subsidence history of the Hawaiian Islands: J. Geophys. Res. 94, 10473-10500, doi:10.1029/JB094iB08p10473, 1989.

Appendix A: (Calculation of required wind speed)

All equations can be found in Le Roux (2005).

Shell density (calcite): ρ_s = 2.85 g cm^{-3}.

Shell shape: Ellipsoid, long axis = 1 cm, intermediate axis = 0.75 cm, short axis = 0.35 cm.

Nominal diameter: $D_n = \sqrt[3]{(1)(0.75)(0.35)}$ = 0.64 cm

Water density: $\rho_w = 0.9982$ g cm^{-3}.

Water dynamic viscosity: $\mu_w = 0.01$ g cm^{-1} s^{-1}.

Air density: ρ_a = 0.0012 g cm^{-3}.

Submerged density of shell in water: $\rho_\gamma = \rho_s - \rho_w = 2.85 - 0.9982 = 1.8518$ g cm^{-3}.

Acceleration due to gravity: g = 981 cm s^{-2}.

Dimensionless grain size (water): $D_{ds} = D_n . \sqrt[3]{\frac{\rho g \rho_\gamma}{\mu^2}} = 0.64 . \sqrt[3]{\frac{(0.9982)(981)(1.8518)}{(0.01)^2}} = 168.14$.

Dimensionless settling velocity of nominal sphere in water:

$W_{ds} = \sqrt{2.531 D_{ds} + 160} = \sqrt{(2.531)(168.14) + 160} = 24.2$.

Real settling velocity of nominal sphere in water:

$$W_s = \frac{W_{ds}}{\sqrt[3]{\rho^2 / \mu g \rho_\gamma}} = \frac{24.2}{\sqrt[3]{(0.9982)^2 / (0.01)(981)(1.8518)}} = 63.69 \text{ cm s}^{-1}.$$

Real settling velocity of ellipsoid:

$$W_e = -W_s\left\{0.572\left[1-\left(\frac{D_i}{D_l}\right)\right]^{2.5} - 1\right\} = -63.69\left\{0.572\left[1-\left(\frac{0.75}{1}\right)\right]^{2.5} - 1\right\} = 62.55\ \text{cm s}^{-1}$$

Dimensionless settling velocity of ellipsoid in water:

$$W_{de} = W_e\sqrt[3]{\rho^2 / \mu g \rho_\gamma} = 62.55\sqrt[3]{(0.9982)^2 /(0.01)(981)(1.8518)} = 23.76$$

Dimensionless critical shear stress in air for W_{de} >11, assuming that β_c levels off as in water:

$$\beta_c = 0.00664\log_{10} W_{de} + 0.00936 = (0.00664)(1.3758) + 0.00936 = 0.0185$$

Critical shear velocity U_{*c} in air:

$$U_{*c} = \sqrt{\frac{\beta_c g D \rho_\gamma}{\rho}} = \sqrt{\frac{(0.0185)(981)(0.64)(2.85-0.0012)}{0.0012}} = 166\ \text{cm s}^{-1}.$$

Assuming a fully rough boundary, required wind speed measured 10 m above the ground:

$$U_a = U_{*c}\left[2.5\ln\left(\frac{y}{D}\right)+8.5\right] = 166\left[2.5\ln\left(\frac{1000}{0.64}\right)+8.5\right] = 4462.9\ \text{cm s}^{-1} \approx 160\ \text{km hr}^{-1}.$$

Table 1. Radiocarbon dates for gastropods from RCI

Table 1. Radiocarbon dates for gastropods from Robinson Crusoe Island

Site	Sample	Lab. Number	Conventional radiocarbon age (yBP)	C13/C12 ratio	Calibrated age (Cal yBP) 2σ	Reservoir corrected age Delta-R= 313±76	Calibrated age (Cal yBP) 2σ	Material	Elevation m a.s.l.
5	PS-25-1	Beta-326738-F	6790±40	-10.8	7680-7580	6480±90	7507-7165	*Fernandezia*	85.0804
1	PS-25-7	Beta-326739-R	7860±40	-8.0	8320-8030	7550±90	8508-8050	*Nerita*	69.7153
1	PS-25-7	Beta-307410-F	4580±30	-8.4	5440-5090	4270±80	4965-4522	*Succinea*	69.7153

Data obtained at Beta Analytic Inc., Miami, Florida

Elevation computed from dGPS data with correction for daily variation of sea level and local height of the antenna

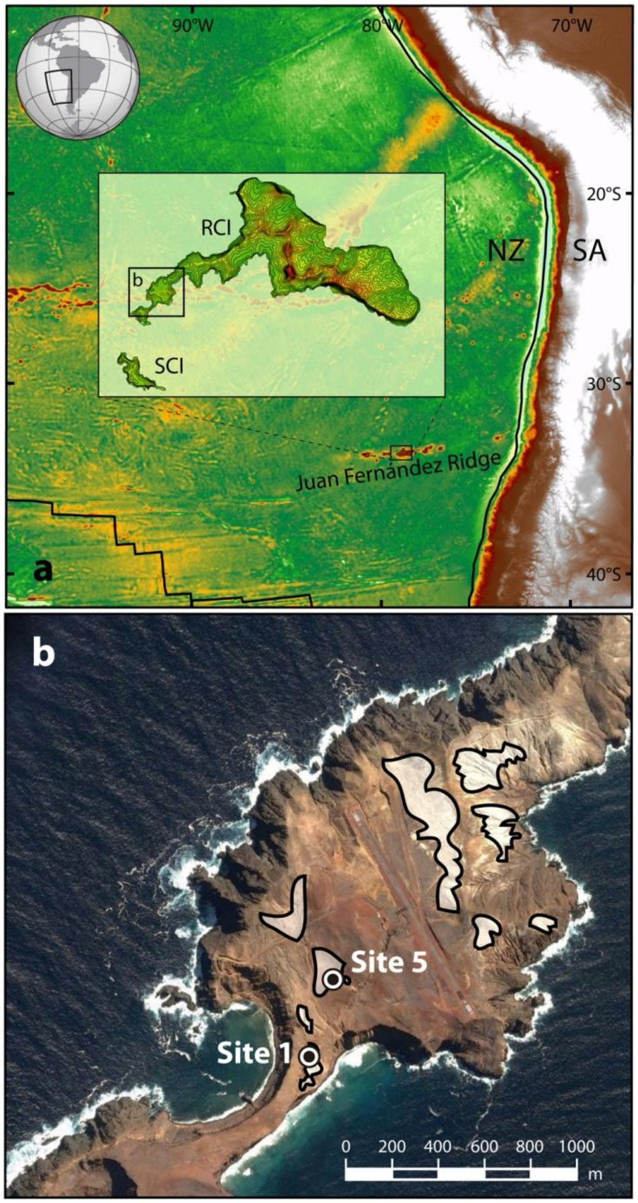
90°W
80°W
70°W
20°S
30°S
40°S
RCI
b
SCI
NZ
SA
Juan Fernández Ridge
a
b
Site 5
Site 1
0 200 400 600 800 1000
m

Figure 1. Location of Juan Fernández Ridge (a), with Robinson Crusoe Island (RCI) and Santa Clara Island (SCI) in a box. Below (b) is a satellite image of the southwestern "panhandle" where the aerodrome is situated. White areas are those of the Bahía Tierra Blanca succession, where a well-exposed supratidal Holocene sequence was dramatically uplifted (see text for details). Sampling sites labeled with numbers (see Table 1). NZ: Nazca Plate: SA: South American Plate.

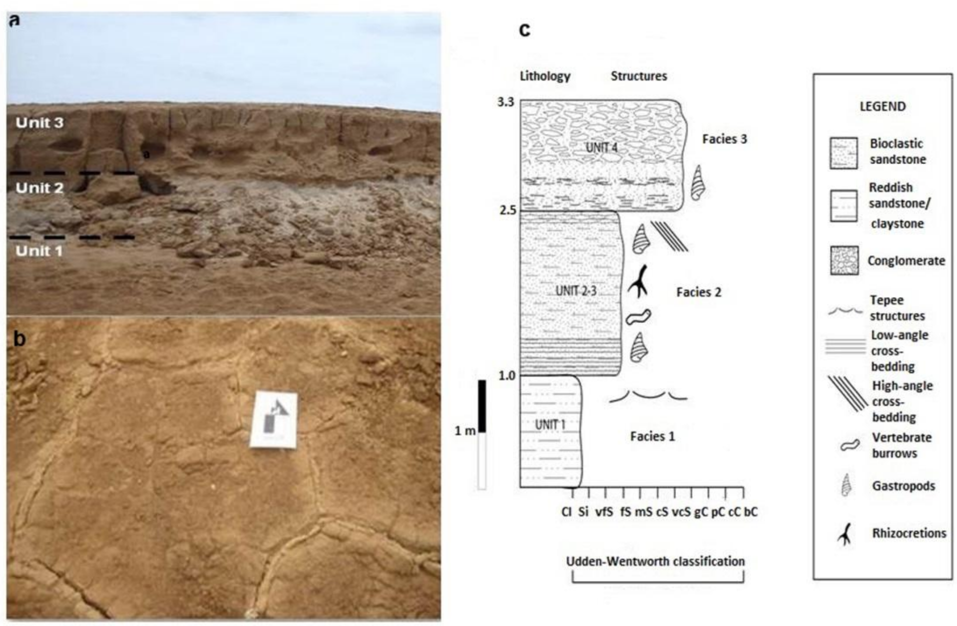

Figure. 2. Exposure of sedimentary units as described in text (a). *Nerita* dated at ca. 8,000yrs BP sampled from Unit 1. Below are 'teepee' structures in Unit 1 (b), interpreted as part of a former supratidal flat. A composite stratigraphic column (c) from records at sites shown in Figure 1.

Figure 3. *Nerita* shells found in eolian deposits of Unit 2. These are marine species, probably incorporated into dunes developed close to the supratidal flat shoreline. Visual field is 2.5 cm.